Available online at www.sciencedirect.com
SCIENCE DIRECT®
International Journal of Mass Spectrometry 235 (2004) 145–154
International Journal of Mass Spectrometry
www.elsevier.com/locate/ijms

Cation–π interactions in gaseous ω-phenylalkyloxonium ions

Barbara Chiavarino*, Maria E. Crestoni, Simonetta Fornarini

Dipartimento di Studi di Chimica e Tecnologia delle Sostanze Biologicamente Attive
Università di Roma "La Sapienza" Piazzale A. Moro 5, I-00185 Rome, Italy

Received 25 March 2004; accepted 21 April 2004

Dedicated to the memory of our mentor, Professor Fulvio Cacace.

Available online 1 June 2004

Abstract

The gas phase reactivity behavior of ω-phenylalkyloxonium ions obtained by protonation or alkylation of ω-phenylalkanols ($C_6H_5(CH_2)_nOH$ with $n = 1$–5, denoted as **1**–**5**, respectively) has been investigated by FT–ICR mass spectrometry and by a radiolytic approach operating at nearly atmospheric pressure. The radiolytic methylation reaction is directed exclusively at the O-atom, yielding oxonium ions whose reactivity behavior varies along the series **1**–**5**. The oxonium ions from the lower members (**1**, **2**) are prone to undergo a nucleophilic displacement process in competition with an exothermic deprotonation reaction at variance with the higher members which are unreactive towards this process. This feature is paralled by their increased stability towards CI(i-C_4H_{10}) induced dissociation, both effects assigned to the increased stabilization gained by the electrostatic interaction of the oxonium part with the π-electron density of the phenyl group allowed by the folding of the aliphatic chain. The occurrence of cycloalkylation processes and peculiar extent of H/D exchange sequences within protonated **3**–**5** lend support to this effect.

Keywords: Gas-phase reactions; Non-covalent interactions; H/D exchange processes; Reaction mechanisms; Cations

1. Introduction

The paramount role played by non-covalent interactions, including van der Waals interactions and hydrogen-bonding, is well documented in all areas of chemistry. Although they are classified as "weak" interactions with respect to covalent bond, they are substantial in molecular recognition mechanisms. Recently, considerable attention has focussed on two different demonstrations of non-covalent interactions, namely the cation–π interactions [1] and non-conventional hydrogen bonds [2]. In both cases the π-electron density of an aromatic ring can be involved, binding either a cation or a hydrogen atom supplied by a hydrogen bond donor, respectively. The cation–π interactions are common in protein structures and in crystal packing. They may affect the formation of host–guest complexes directing protein-ligand [3] or substrate–enzyme binding and the operation of ion channels and can be exploited in the design of synthetic ionophores [4] and model receptors [5]. A wide range of cations can be involved in cation–π interactions including simple metal ion such as Na^+ and K^+, the most abundant cations in living systems. Cation–π interactions are affected by the environment [6] and their features have been probed in the gas phase by computational [7] and/or mass spectrometric studies [8]. Pioneering mass spectrometric experiments on the Li^+/benzene and K^+/benzene association are due to Beauchamp [9] and Kebarle [10], respectively. Electrostatic interactions are dominant in prototypical cation–π interactions [1a]. A significant contribution may be due to the polarization of the π-electron system by the cation as shown by theoretical calculations [3a,11] and cation induced polarization and coiling of an alkyl chain has been suggested to account for the enhanced Li^+ binding energies of alkylbenzenes [12]. It has been suggested that the aromatic residues on the side chains of amino acids can stabilize carbocation intermediates in enzymatic reactions. However, the gas phase reaction of carbenium ions with benzene, leading to the formation of a σ-complex, does not necessarily proceed by a distinct π-complex intermediate [13]. On the other hand, ammonium ions, which are coordinatively saturated,

* Corresponding author. Tel.: +39-06-49913634; fax: +39-06-49913602.
E-mail address: barbara.chiavarino@uniroma1.it (B. Chiavarino).

1387-3806/$ – see front matter © 2004 Elsevier B.V. All rights reserved.
doi:10.1016/j.ijms.2004.04.008

can bind to the π-electrons of aromatic systems according to the same fundamental interactions that operate for alkali metal ions although hydrogen bonding interactions, both NH-aromatic π-system and CH-aromatic π-system, are conceivable [14]. Indeed, the π-electron density of aromatic systems is widely recognized to perform as hydrogen bond acceptor even towards neutral donors [2,15]. An interesting example of the role played by non-covalent interactions is shown by the protonated benzene–water cluster. According to ab initio calculations the H_3O^+–benzene complex is energetically favored by 10.9 kJ/mol with respect to the $C_6H_7^+$–water complex, in spite of the fact that benzene is 56.4 kJ/mol more basic than water in the gas phase [16]. This finding arises from the substantial binding energy of the H_3O^+–benzene complex with the respect to the corresponding value for $C_6H_7^+$–water complex. The calculated geometry of H_3O^+–benzene resembles an edge-on π-complex with an O-bound hydrogen interacting with the π-electron density above a C–C bond. This remarkably stable non-covalent complex combines the features of a cation–π interaction with the directional character of a hydrogen bond belonging to the so-called uncoventional type. The strong stabilization exhibited by the H_3O^+ association with benzene is expected to affect the reactivity behavior of gaseous oxonium ions whenever the molecular environment allows them to approach the π-electron density of an aromatic ring. Suitable systems to verify any possible role played by the interaction of a cation with the π-electron density of an aromatic ring may be devised where the cationic site is covalently bound to a phenyl ring by means of a aliphatic chain. Several studies have addressed the reactivity and thermodynamic features of the cationic intermediates obtained from the addition of a gaseous electrophile (E^+) to one phenyl ring of α,ω-diphenylalkanes (DPA) [13c–d,17]. In the first place, the presence of two phenyl rings confers enhanced stabilization to the E^+-DPA collision complex, due to E^+ interacting simultaneously with the π-electron densities of both phenyl groups. Secondly, in the ensuing arenium ion the participation of the spectator ring is clear by the role played in stabilizing the π-adduct [17b] and in reacting with it by proton and group transfer processes. The same approach has been used to investigate the effect exerted by a neighbouring phenyl group on the formation and reaction of an oxonium ion obtained by E^+ attack to ω-phenylalkanols aiming to point out the role of possible intramolecular interactions between the π-electron density and the oxonium part of the molecule. It may be expected that the spatial requirements for the two groups to interact will vary along the investigated series of compounds, namely $C_6H_5(CH_2)_nOH$ (ROH) with $n = 1$–5, henceforth denoted as **1**–**5**, respectively. Where the conformation of the ions is suitable to establish a hydrogen–π (or generally cation–π) interaction, their stability is expected to be greater. The investigation was effected in the gas phase, an environment free of solvation and ion pairing effects, typical of the condenses phase. Two different and complementary methodologies were exploited, namely a radiolytic technique [18] and FT–ICR mass spectrometry [19].

2. Experimental section

2.1. Materials

The gases used (O_2, i-C_4H_{10}) were research grade products from Rivoira Co. with a stated purity exceeding 99.95 mol%. MeF, supplied by H&S Chemical, was 99.8 mol% pure. Bis-[(3-phenyl)-propyl]ether and bis-[(2-phenyl)-ethyl]ether to be used as GC standards were prepared by the reaction of a sodium alkoxide, $C_6H_5(CH_2)_{2,3}ONa$, with the alkyl halide $C_6H_5(CH_2)_{2,3}Br$. All other chemicals used were obtained from commercial sources.

2.2. Radiolytic experiments

The gaseous samples were prepared in sealed 250 ml Pyrex vessels using standard vacuum procedures. Because an accurate knowledge of the relative amounts of the reactants was required, carefully weighted combinations of the substrate and additive were prepared and an equilibration time (1 h at 150 °C) was allowed to assure their complete vaporization. The irradiations, run to less than 1% of substrate conversion, were performed in a 220 Gammacell (Nuclear Canada Ltd.) for 3 h at the dose rate of ca. 10^{-4} Gy/h in a thermostated device. The radiolytic products were extracted by freezing the vessels at 77 K and then washing the inner walls with ethanol by repeated freeze–thaw cycles. The identity of the products was checked with reference standards, (some of them obtained by synthesis) and their yields were obtained by GC–MS analysis using a Hewlett-Packard 5890 series II gas chromatograph in line with a quadrupole HP 5989B mass-spectrometer. The fused silica column (50 m long, 0.20 mm i.d.) coated with a 0.5 μm cross-linked methylsilicone phase (HP PONA column) was operated isothermally at 100 °C for 2 min and then heated at the rate of 8 °C/min to 150 °C and then at 16 °C/min to 240 °C. Blank experiments were done to ascertain the radiolytic origin of products.

2.3. FT–ICR mass spectrometric experiments

The FT–ICR experiments were performed with a Bruker Spectrospin Apex 47e spectrometer equipped with an external ion source and a cylindrical "infinity" cell of 6 cm length and 6 cm diameter situated between the poles of a 4.7 T superconducting magnet. $[M + H]^+$ and $[M + H - H_2O]^+$ ions were generated by the chemical ionization (CI) of a selected substrate (M) in the external ion source using i-C_4H_{10} as reactant gas at the pressure of ca. 6×10^{-5} mbar and transferred into the cell. The ions of interest were isolated by broad band ejection of any other unwanted ion and mass

spectra were acquired at increasing reaction times, showing the progress of the reaction with a neutral reagent introduced by a needle valve to a constant pressure in the range of 4×10^{-8} to 9×10^{-8} mbar. Inlets and cell were at room temperature (25 °C), which is considered as the effective reaction temperature. The pseudo-first order rate constants (k_{exp}) of the ion-molecule reactions were derived from the exponential decay of the reactant ion abundance as a function of time and converted to absolute rate constants using the known neutral pressure. The partial pressures were read from a calibrated ion gauge and corrected by individual response factors [20]. The reported values of second-order rate constants are the average of usually three experiments run at different neutral pressures. The normalized efficiency (in %) of the ion–molecule reaction is given by k_{exp}/k_{coll}. The collision rate constant (k_{coll}) was calculated using the parametrized trajectory theory [21].

3. Results

3.1. Radiolytic reactions

The reactivity of the homologue series of ω-phenylalkanols **1**–**5** towards Me_2F^+ ions, powerful methylating agents obtained from the radiolysis of MeF according to a well-known sequence of ionic processes [22], was studied in the gas phase at nearly atmospheric pressure. Features of the reaction conditions that may affect the product pattern were investigated, namely the presence at variable concentration of an added base (triethylamine, TEA), the relative amounts of the gaseous components, and the temperature of the experiments.

Table 1 summarizes the composition of the irradiated systems and the reaction products whose ionic origin is ensured by the presence of a large excess (15 mbar) of O_2, introduced as an efficient alkyl radical scavenger. The absolute radiochemical yields, measured by their G_{+M} value, are found to be close to the known G_{+M} value of the reactant ion and decrease with the increasing concentration of the base, a trend that is typically observed for products originating from positively charged electrophiles, thus testifying their ionic origin.

Although aryl alcohols own two sites potentially suitable to be attacked by an electrophilic cation, the aromatic ring and the hydroxyl oxygen, only the oxygen methylation product, ROMe in Table 1 (R = $Ph(CH_2)_n$–, where *n* equals the number of methylene units in the reagent substrate), is observed. When **1** and **2** are used as substrates, the corresponding symmetrical ether products are also formed, ROR. In each set of experiments run at constant temperature the relative yields of the two ether products, ROMe and ROR, are found to depend on the ratio between the concentration of the added base and the substrate concentration, [TEA]/[ROH]. For example, at 100 °C the formation of ROR from **2** appears favored as the TEA concentration decreases, varying from 20% of the overall ether products when no base is added to 5% when the [TEA]/[ROH] ratio approaches two. The same trend is confirmed at 160 °C. Experiments run at a constant value of [TEA]/[ROH] show that the formation of ROR is favored at higher temperature. For example, when [TEA]/[ROH] = 0.6 the relative fraction of ROR obtained at 160 °C is about three times the amount found at 100 °C, in the case of **2**. The formation of ROR from **1** is comparatively more extensive than from **2**. As in the latter case, the relative

Table 1
Gas-phase reaction of Me_2F^+ with ω-phenylalkanols (ROH)

System composition (mbar)[a]			*T* (°C)	[TEA]/[ROH]	Products (%)[b]	
ROH	TEA	MeF			ROMe	ROR
1 (2.8)	1.1	585	100	0.38	54	46
1 (2.6)	1.6	585	100	0.61	60	40
1 (2.1)	1.6	565	100	0.76	66	34
1 (2.3)	2.1	585	100	0.91	67	33
1 (1.6)	1.7	585	100	1.1	74	26
1 (1.5)	2.0	595	100	1.33	78	22
1 (0.87)	1.3	585	100	1.50	80	20
1 (0.62)	1.1	585	100	1.8	82	18
1 (1.9)	1.3	590	150	0.65	28	72
1 (1.4)	1.1	590	150	0.81	32	68
1 (1.5)	1.5	590	150	1.0	33	67
1 (1.1)	1.4	590	150	1.2	30	70
1 (1.3)	1.9	580	150	1.4	29	71
1 (1.3)	2.1	575	150	1.6	31	69
1 (1.2)	2.2	590	150	1.8	33	67
1 (1.5)	3.0	575	150	2.0	34	66
2 (2.4)	–	560	100	0	80	20
2 (3.0)	0.64	585	100	0.21	87	13
2 (1.8)	0.58	575	100	0.33	89	11
2 (2.3)	0.91	580	100	0.39	85	15
2 (2.0)	1.2	590	100	0.61	91	9
2 (1.7)	1.5	585	100	0.86	91	9
2 (1.5)	1.4	585	100	0.95	92	8
2 (0.70)	1.2	575	100	1.7	95	5
2 (2.4)	0.95	585	160	0.40	71	29
2 (2.6)	1.1	580	160	0.43	69	31
2 (1.9)	1.1	575	160	0.61	67	33
2 (3.1)	2.6	590	160	0.85	76	23
2 (2.0)	2.0	585	160	0.98	74	26
2 (2.4)	3.2	575	160	1.3	79	21
2 (1.0)	1.5	570	160	1.5	86	14
2 (0.83)	1.4	585	160	1.7	85	15
2 (0.90)	1.8	575	160	1.9	87	13
3 (1.7)	–	585	100	0	100[c]	n.d.
3 (2.3)	0.92	565	100	0.41	100[c]	n.d.
3 (1.7)	–	585	160	0	100[c]	n.d.
3 (2.3)	0.88	590	160	0.38	100[c]	n.d.
4 (2.5)	–	585	100	0	93[d]	n.d.
4 (2.2)	0.92	575	100	0.42	97[d]	n.d.
4 (2.1)	–	570	150	0	94[d]	n.d.
4 (2.5)	0.88	595	150	0.36	95[d]	n.d.
5 (1.6)	–	625	100	0	100[e]	n.d.

[a] All gaseous systems contained O_2 (15 mbar) as radical scavenger.
[b] Average error ± 10%.
[c] Indane is not detected among the reaction products.
[d] Tetraline is formed accounting for a yield complementary to 100.
[e] Benzosuberane is not detected among the reaction products.

yields of ROMe and ROR depend on the relative amount of base with respect to substrate, at least at 100 °C where the fraction of ROR varies from 46 to 18%, in response to a change of the [TEA]/[ROH] ratio from 0.38 to 1.8. At higher temperature, 150 °C, ROR (R = $PhCH_2$–) becomes the major product, with a relative yield that appears constant at ca. 70% in the [TEA]/[ROH] range spanning from 0.65 to 2.0.

ROR is not detected among the products of the higher alcohols, **3**–**5**, even in the experiments run at higher temperature (150–160 °C) in the absence of any added base. However, in the reaction of **4** the formation of ROMe is accompanied by minor amounts of tetraline. The yield of this side product seems to be positively affected by decreasing amine concentration and increasing temperature, though the observed change is barely appreciable.

3.2. Mass spectrometry

3.2.1. CI product patterns

Ionization of **1**–**5** under CI(i-C_4H_{10}) condition was performed in the external ion source of the FT–ICR instrument at a total pressure about seven orders of magnitude lower than that prevailing in the radiolytic experiments. The results are reported in Table 2. As in the radiolytic experiments, the homologue series of substrates **1**–**5** show a different behavior upon protonation by Me_3C^+ ions, depending on the size of the alkyl chain. In fact, CI(i-C_4H_{10}) of **1** and **2** yields ions at m/z 91 and 105, respectively, as the major product ions. These ions, formally corresponding to $PhCH_2^+$ and $PhC_2H_4^+$, may arise by loss of one molecule of water following the protonation of the OH group, as depicted in Eq. (1).

$$\mathrm{ROH} \overset{+\,\mathrm{Me_3C^+}}{\underset{-\,i\text{-}\mathrm{C_4H_8}}{\rightarrow}} [\mathrm{ROH_2}^+] \rightarrow \mathrm{R}^+ + \mathrm{H_2O} \qquad (1)$$

Although the process of water loss is observed also in the protonation of the higher homologues, the most prominent ion obtained by CI(i-C_4H_{10}) of **3**–**5** is the intact protonated molecule, $[ROH + H]^+$. The corresponding $[ROH + H]^+$ ions are not observed in the case of **1** and **2**.

Table 2
Product ions from the CI(i-C_4H_{10}) of ω-phenylalkanols (ROH)

ROH	Product ions (%)
1	$[PhCH_2]^+$ (85); $[C_4H_9–C_7H_6]^+$ (15)
2	$[Ph(CH_2)_2]^+$ (81); $[Ph(CH_2)_2OH]^+$ (9); $[C_4H_9–C_8H_8]^+$ (7); $[C_4H_9–C_8H_9OH]^+$ (3);
3	$[Ph(CH_2)_3OH]H^+$ (65); $[Ph(CH_2)_3]^+$ (15); $[Ph(CH_2)_3OH]_2H^+$ (20)
4	$[Ph(CH_2)_4OH]H^+$ (44); $[Ph(CH_2)_4]^+$ (26); $[Ph(CH_2)_4OH]_2H^+$ (30)
5	$[Ph(CH_2)_5OH]H^+$ (41); $[Ph(CH_2)_5]^+$ (29); $[PhCH_2]^+$ (17); $[PhC_2H_4]^+$ (6); $[PhC_3H_6]^+$(7)

Table 3
Rate constants (k_{exp}) and efficiences (Eff) of the reactions of protonated ω-phenylalkanols 3–5 and related ions with MeOD

Substrate ion[a]	k_{exp}[b]	Eff (%)[c]	Product ions
$[Ph(CH_2)_3OH]H^+$	3.2	22	$C_9H_{12}OD^+ \rightarrow C_9H_9OD_4^+$
$C_9H_{11}^+$ (**3**)	–	–	unreactive
$C_9H_{11}^+$ (indane)	3.1	21	$C_9H_{10}D^+ \rightarrow C_9H_6D_5^+$
$[Ph(CH_2)_4OH]H^+$	3.3	23	$C_{10}H_{14}OD^+ \rightarrow C_{10}H_{11}OD_4^+$
$C_{10}H_{13}^+$ (**4**)	2.9	20	$C_{10}H_{12}D^+ \rightarrow C_{10}H_8D_5^+$
$C_{10}H_{13}^+$ (tetraline)	2.7	18	$C_{10}H_{12}D^+ \rightarrow C_{10}H_8D_5^+$
$[Ph(CH_2)_5OH]H^+$	3.0	21	$C_{11}H_{16}OD^+ \rightarrow C_{11}H_{13}OD_4^+$
$C_{11}H_{15}^+$ (**5**)	2.3	16	$C_{11}H_{14}D^+ \rightarrow C_{11}H_{10}D_5^+$
$C_{11}H_{15}^+$ (benzosuberane)	3.0	21	$C_{11}H_{14}D^+ \rightarrow C_{11}H_{10}D_5^+$
$[Ph(CH_2)_3OCH_3]H^+$	0.15	1.0	$C_{10}H_{14}OD^+$
$[Ph(CH_2)_2CH_3]H^+$	3.2	22	$C_9H_{12}D^+ \rightarrow C_9H_7D_6^+$

[a] The substrate ions are obtained by CI(i-C_4H_{10}) of a neutral substrate (given in parentheses when ambiguity may exist) in the external ion source of the FT–ICR mass spectrometer.
[b] In units of 10^{-10} cm^3/molecule. Estimated error ± 30%.
[c] The normalized efficiency Eff = k_{exp}/k_{coll}, was calculated as described in the experimental section.

3.2.2. Kinetics of the ionic reactions

In order to characterize the ions obtained by protonation of **3**–**5**, their H/D exchange reactivity with MeOD has been assayed in the FT–ICR cell. The product ions, the rate constants and the efficiencies of these reactions, together with those of protonated benzocycloalkenes used as reference ions, are listed in Table 3. In each of these experiments, the selected ion is allowed to react with a stationary concentration of MeOD to observe any potential H/D exchange processes. All the ions corresponding to the protonated substrate ($[ROH + H]^+$ ROH = **3**–**5**) show similar reactivity towards MeOD. This neutral promotes sequential deuterium incorporation into the protonated substrates, ending with the incorporation of four deuterium atoms in each case. Fig. 1 shows an exemplary reaction profile along with best fitting

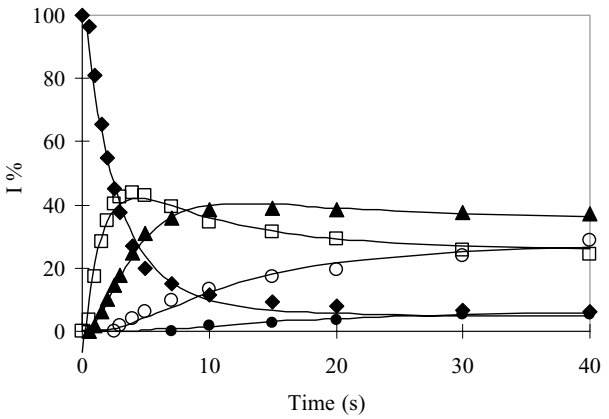

Fig. 1. Time dependence of the normalized abundances of the ions formed upon reaction of $[Ph(CH_2)_3OH]H^+$ ions m/z 137 formed by CI(i-C_4H_{10}) of **3** in the presence of MeOD at 5.8×10^{-8} mbar (ions m/z 137 (◆), m/z 138 (□), m/z 139 (▲), m/z 140 (O), m/z 141 (●).

curves obtained by the Kinfit program [23] for the reaction of the consecutive incorporation of deuterium atoms in protonated **3** with MeOD, at the apparent neutral pressure of 5.8×10^{-8} mbar.

Also the ions resulting by water loss from protonated **3–5** were assayed by H/D exchange with MeOD. A different behavior characterized the ions $C_9H_{11}^+$, $C_{10}H_{13}^+$, and $C_{11}H_{15}^+$ generated in the external ion source by CI(*i*-C_4H_{10}) of **3–5**, respectively. Whereas $C_9H_{11}^+$ is unreactive in presence of MeOD, H/D exchange processes are observed when $C_{10}H_{13}^+$ or $C_{11}H_{15}^+$ are allowed to react, ending with the incorporation of five D-atoms within both of these ions. The sequence of five H/D exchange processes is also observed when MeOD is allowed to react with the $C_9H_{11}^+$, $C_{10}H_{13}^+$, and $C_{11}H_{15}^+$ ions generated by protonation of the corresponding cycloalkanes, viz. indane, tetraline and benzosuberane, respectively. Also, the rate constants for the decay of the substrate ion are equal within experimental error both for $C_{10}H_{13}^+$ ions (irrespective of their formation by water loss from protonated **4** or by protonation of tetraline) and for $C_{11}H_{15}^+$ ions (irrespective of their formation by water loss from protonated **5** or by protonation of benzosuberane).

Table 4
Individual rate constants for the consecutive steps of the H/D exchange reaction between selected ions and MeOD in the FT–ICR cell, obtained with the KinFit program [23]

Substrate ion[a]	k_1[b]	k_2[b]	k_3[b]	k_4[b]	k_5[b]	k_6[b]
$[Ph(CH_2)_3OH]H^+$	4.6	2.5	0.58	0.42	–	–
	6.9	*7.5*	*0.9*	*1.2*	–	–
$[Ph(CH_2)_4OH]H^+$	3.6	2.1	0.26	0.15	–	–
	5.4	*6.3*	*0.40*	*0.45*	–	–
$[Ph(CH_2)_5OH]H^+$	3.6	2.3	0.74	0.64	–	–
	5.4	*6.9*	*1.1*	*1.9*	–	–
$C_9H_{11}^+$ (indane)	4.1	3.3	2.6	1.7	0.62	–
	5.0	*5.0*	*5.2*	*5.1*	*3.7*	–
$C_{10}H_{13}^+$ (**4**)	4.1	3.3	3.0	2.0	0.58	–
	5.0	*5.0*	*6.0*	*6.0*	*3.5*	–
$C_{10}H_{13}^+$ (tetraline)	4.2	3.4	3.0	2.1	0.82	–
	5.0	*5.1*	*6.0*	*6.3*	*4.9*	–
$C_{11}H_{15}^+$ (**5**)	3.4	2.8	2.4	1.7	0.64	–
	4.1	*4.2*	*4.8*	*5.1*	*3.8*	–
$C_{11}H_{15}^+$ (benzosuberane)	3.0	2.3	2.0	1.2	0.63	–
	3.6	*3.5*	*4.0*	*3.6*	*3.8*	–
$[Ph(CH_2)_2CH_3]H^+$	4.8	4.3	3.1	2.2	1.3	0.82
	5.6	*6.0*	*5.5*	*5.2*	*4.6*	*5.8*

[a] The substrate ions are obtained by CI(*i*-C_4H_{10}) of a neutral substrate (given in parentheses when ambiguity may exist) in the external ion source of the FT–ICR mass spectrometer.

[b] In units of 10^{-10} cm^3/molecule. The rate constants[b] reported in italics are corrected by statistical factors accounting for the probability of H^+ vs. D^+ transfer in the elementary step within the framework of the proposed H/D exchange scheme (see text).

Model ions obtained by protonation of $Ph(CH_2)_3OMe$ are found to undergo slow exchange of only one hydrogen whereas protonated *n*-propylbenzene exchanges six hydrogens in a relatively fast stepwise sequence.

The rate constants for the individual steps of the H/D exchange sequences were determined from a best fitting of the plots describing the time dependence of ion abundances using the Kinfit program [23] and are reported in Table 4. The kinetic pattern comprises a sequence of stepwise, reversible reactions of incorporation of D atoms.

4. Discussion

4.1. The methylation process

A measure of the methylating power of Me_2F^+ ions is given by the methyl cation affinity (MCA) of MeF, namely the reaction enthalpy for the dissociation of a methyl cation from Me_2F^+ (Eq. (2)) [24].

$$Me_2F^+ \rightarrow MeF + Me^+$$
$$\Delta H_2^o = MCA(MeF) = 51\,kcal\,mol^{-1} \quad (2)$$

This value should be compared with the MCA of the selected substrate. The exothermicity of the reaction is given by the difference in MCA between MeF and the ω-phenylalkanol, as shown in Eq. (3).

$$Me_2F^+ + ROH \rightarrow MeF + [ROH + Me]^+$$
$$\Delta H_3^o = MCA(MeF) - MCA(ROH) \quad (3)$$

As stated above, ω-phenylalkanols have two different types of nucleophilic sites, namely the hydroxyl oxygen and the individual positions of the aromatic ring (Scheme 1), each site being characterized by a specific MCA value.

The radiolytic product pattern shows that the methylation on the hydroxyl oxygen does indeed occur. The MCA's of the phenyl alkanols are not known, but the MCA value of MeOH (334 kJ/mol) [24b] and the estimated value of 355 kJ/mol for benzene provide a reference for the relative

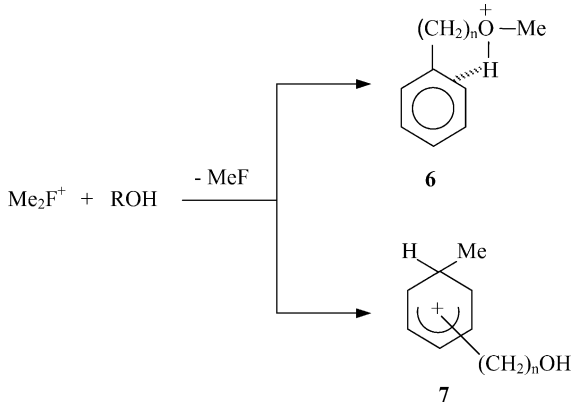

Scheme 1.

energetics of the methyl cation attachment at the hydroxyl and the phenyl moiety of the selected substrates. The estimated MCA value of benzene was evaluated considering the heat of formation of ipso-protonated toluene, the primary product ion from the methylation of benzene. H_f^o of *ipso*-protonated toluene is obtained from the experimental proton affinity (PA) of toluene (784 kJ/mol) [25a] corresponding to the formation of the most stable *para*-protonated isomer, taking account the difference in stability between the two isomers as obtained by ab initio calculations [25b]. The thermochemical data for the methylation of methanol and benzene by Me_2F^+ ions are expected to be lower limits for the values pertaining to methylation at the oxygen atom and at the aromatic ring of $Ph(CH_2)_nOH$, respectively, because the stabilization effects of a $Ph(CH_2)_{n-1}$ group on the MCA of methanol and of a $HO(CH_2)_n$ substituent on the MCA of benzene are not considered. However, the benzene and methanol MCA data suggest that the methylation at the aryl moiety of $Ph(CH_2)_nOH$ is favored by 21 kJ/mol with respect to *O*-methylation, a rather small bias. This difference may be easily counterbalanced by specific structural effects due to interactions arising between the methylated charged moiety with the second functional group in the molecule. In fact, when the methylation occurs on the hydroxyl oxygen, the so formed species (**6**) can be stabilized by interaction of the oxonium end with the aromatic ring. Similarly, the methylated arenium end of **7** may be stabilized by interaction with the OH group. The protonated benzene–water complex provides a simplified model showing that non-covalent interactions largely favor the H_3O^+–benzene complex [16]. As described in the introduction, ample evidence testifies the intramolecular stabilization provided to a cationic site by an aryl group bound by a flexible aliphatic chain. Thus, this kind of electrostatic stabilization, an intramolecular cation–π interaction, may conceivably revert the expected order of MCA values of the two nucleophilic ends of the ω-phenylalkanols.

The selective *O*-methylation can be explained also by a kinetic factor. In the methyl cation transfer reaction from Me_2F^+ to the aryl group, the nucleophilic site, a delocalized π system, undergoes a major electronic and structural reorganization in order to build a $Me–C_{aryl}$ bond. The resulting significant activation barrier is responsible for example for the slow kinetics of the methylation of benzene by Me_2Cl^+ ions, in spite of its exothermicity [26]. On the other hand, a relatively minor activation energy barrier is expected for the methylation at the oxygen atom where the lone pair electrons are readily available to build the O–Me bond.

4.2. The radiolytic methylation of *1*–*5*

The formation of ROMe as the exclusive radiolytic methylation product of **1**–**5** shows that the active methylation site is the oxygen atom. Although this finding is a common feature for the homologue series, at closer inspection significant reactivity differences among its members can be traced, obviously depending on the varying length of the aliphatic chain. The *O*-methylation product is formed by an exothermic alkylation process, yielding primarily an excited $RO^+(H)Me$ ion. The excess energy can be released to the bulk MeF molecules before undergoing further reaction, by unreactive thermalizing collisions in the gaseous environment at atmospheric pressure. The thermalized oxonium ion (**6**) may undergo competitive paths, as illustrated in Scheme 2. It can be deprotonated by an added strong base (B), giving ROMe as neutral end product (pathway a in Scheme 2). TEA was chosen as the base because of its high PA (982 kJ/mol), relative to the reported PA of methyl benzyl ether (819 kJ/mol) [25a]. Considering the high exothermicity of the deprotonation reaction, it is conceivable that TEA deprotonates **6** at each collision with a kinetic constant (k_{B1}) that may be evaluated by ion-molecule collision theories [21]. Also the substrate itself (ROH) may deprotonate the ionic intermediate (**6**), according to a somewhat endothermic and consequently slower reaction (pathway b in Scheme 2) with k_{B2} rate constant. Alternatively, **6** may undergo a nucleophilic substitution reaction by ROH (k_{Nu}, observed only in the reaction of **1** and **2**) where methanol is the leaving group. A symmetric oxonium ion is formed, R_2OH^+ (**8**), finally yielding ROR as neutral product (pathway c in Scheme 2).

Within the framework of Scheme 2, a linear dependence is expected for the relative yields of the two radiolytic products ROMe and ROR on the [B]/[ROH] ratio (Eq. (4), where [B] and [ROH] are the stationary concentrations of TEA and ROH, respectively) with a slope equal to the k_{B1}/k_{Nu} ratio. Linear plots are obtained, as shown in Fig. 2 for the reaction of **1** at 100 °C.

$$\frac{[ROMe]}{[ROR]} = \frac{k_{B1}[B] + k_{B2}[ROH]}{k_{Nu}[ROH]} = \frac{k_{B1}[B]}{k_{Nu}[ROH]} + \frac{k_{B2}}{k_{Nu}} \quad (4)$$

Under the reasonable assumption that the deprotonation of **6** by TEA occurs upon every collision, the rate constant k_{B1} is estimated to be approximately constant for the various substrates whereas the value of k_{Nu} is found to vary when **1** and **2** are used as substrates. The slopes of the linear plots for the methylation reaction of **1** and **2** run at 100 °C, 2.7 and 7.8, respectively, suggest that the nucleophilic substitution is indeed slower than the deprotonation of **6**. Furthermore, the

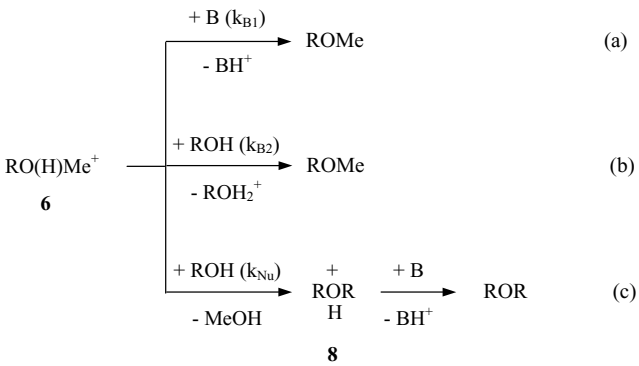

Scheme 2.

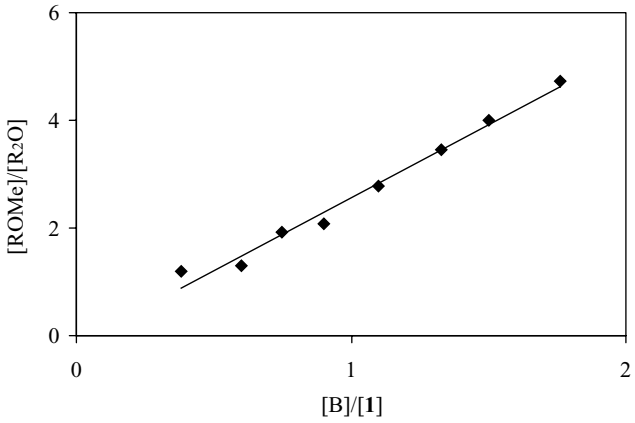

Fig. 2. Plot of the [ROMe]/[R_2O] yield ratio (R = $PhCH_2$–) vs. [B]/[**1**], namely the partial pressure ratio, from radiolytic experiments at 100 °C of benzyl alcohol **1**. Details of individual experiments are listed in Table 1.

nucleophilic displacement is slower when **2** is the reagent substrate.

Apparently, the increasing chain length decreases the efficiency of the nucleophilic substitution reaction. This trend is confirmed by the higher homologues (**3**–**5**) which do not give any ROR product, even in the absence of added base. This behavior can be explained by an increased stability of the ionic intermediate, $RO^+(H)Me$, due to the increasing interaction between the positively charged oxonium end and the aromatic ring allowed by an appropriate folding of the aliphatic chain as the number of the methylene units increases. Due to the presence of an activation barrier, the rate of the nucleophilic substitution reaction is expected to display a positive temperature dependence. Accordingly, the slope of the linear plot obtained for the [ROMe]/[ROR] yield ratio from **2** at 150 °C decreases to 3.3, an effect to be ascribed almost entirely to k_{Nu} because of the minor temperature effect expected on the collisional rate constant for the deprotonation reaction [21]. The behavior of [ROMe]/[ROR] yield ratio from **1** in the methylation reaction run at 100 °C is different, showing little sensitivity to the [B]/[ROH] ratio. This behavior is likely due to the remarkable tendency of the oxonium ion from **1** to undergo fragmentation yielding benzyl cations when given energy by increasing the temperature of the high pressure radiolytic environment, as also shown by the CI(*i*-C_4H_{10}) mass spectra. The benzylation of **1** by free benzyl cations thus becomes an independent source of ROR.

The lack of ROR products from the higher homologues **3**–**5** is accounted for by the intramolecular stabilization gained by the corresponding methylated oxonium ions where the cationic site can approach the phenyl ring. Indeed the occurrence of a folded conformation is responsible for the formation of a cyclization product that is obtained from the reaction of **4**, though in only modest yield. The formation of tetraline (Scheme 3) arises by an intramolecular nucleophilic substitution where C_{ortho} binds to the remote methylene group and MeOH is the leaving group.

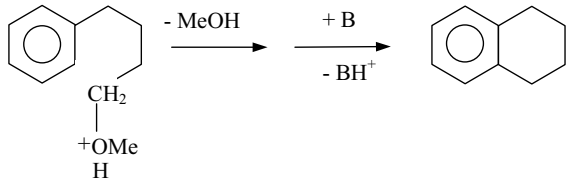

Scheme 3.

The clear tendency to prefer the formation six-membered rings, and thus tetraline-type products, has been reported for the electrophilic cyclization of ω-phenylalkyl-type cations under CI conditions [27].

Even at higher temperature, where the entropically unfavourable folded conformation is expected to be less populated, the intermolecular nucleophilic substitution reaction remains ineffective for **3**–**5**, signifying a decreased reactivity of the oxonium ion **6** towards nucleophilic attack by ROH when the methylene chain is longer. This result can be explained by the increased stabilization of the positive charge by the π system of the spectator aromatic ring. The stabilization comes into play when the methylene chain is long enough (for $n = 3$–5) to allow a proper approach between the charge and the aromatic system.

4.3. The reactivity behavior of **1**–**5** *towards protonation and H/D exchange in FT–ICR mass spectrometry*

The CI(*i*-C_4H_{10}) mass spectra of **1**–**5** show once again a marked difference between **1**–**2** and the higher members of the series. The reagent ion, Me_3C^+, is a mild protonating agent, whose conjugate base is characterized by a PA value close to the one estimated for **1** [25a]. However, in spite of this choice, the protonation of **1** and **2** at 6×10^{-5} mbar leads to the ions formally corresponding to $PhCH_2^+$ and $PhC_2H_4^+$ as major products. Their formation implies the loss of water from an oxonium intermediate ROH_2^+ (Eq. (1)) or, alternatively, the loss of Me_3COH from an intermediate adduct ion, $ROH(CMe_3)^+$. In all cases an intermediate oxonium ion is formed evolving into the dissociation products. The ion can be formed either by direct attack at the OH group or by electrophilic attack at the ring followed by ring to oxygen proton migration, as suggested by the formation of minor products formally corresponding to C_4H_9–$C_7H_6^+$ and C_4H_9–$C_8H_8^+$, from the CI(*i*-C_4H_{10}) of **1** and **2**, respectively. The formation of product ions by loss of water (or Me_3COH) from **1** and **2** under CI conditions is ascribed to the comparatively lower stability of the oxonium intermediates favoring the entropically driven dissociation process in the low pressure environment. It may also reflect a comparatively high stability of the product ions. The protonated species from **3**–**5** are instead stable with respect to dissociation, likely reflecting the stability of a folded conformation where the charged site approaches the electron donating group. Structural information can be obtained by sampling these species by the H/D exchange reaction with

MeOD [28]. Methanol is selected as the exchange reagent in view of its PA value, close to the ones pertaining to the sites possibly involved in the protonation of **3**–**5**, namely the hydroxyl group and the phenyl ring. Protonation on oxygen implies two exchangeable hydrogens on the basic site and is expected to lead to the incorporation of two D atoms according to the reaction pathway exemplified by the first two steps of Scheme 4. Protonation on the phenyl ring leads to an alkyl-substituted arenium ion, prone to undergo exchange of six hydrogens [29], as indeed verified within protonated *n*-propylbenzene (Table 3). Experimentally, the progress of H/D exchange within protonated **3**–**5** ends with the incorporation of four D atoms according to a pattern that can be accounted for by exchange at the oxonium moiety activating two ring positions as well, conceivably the two ortho positions. The proposed 2 + 2 sequence is supported by a kinetic analysis of the H/D exchange reaction. When the rate constants for the individual steps (Table 4) are statistically corrected according to the suggested mechanism, two distinct values are obtained. The first two H/D exchange steps are characterized by a common higher rate coefficient, whereas the remaining two events occur at a similar slower rate, as expected if two different couples of hydrogen atoms are involved. The details of the interaction between the oxonium moiety and the ring hydrogens may once again involve the folding of the aliphatic chain to allow a reversible H^+/D^+ transfer process between the O-atom and the C_{ortho} atom as shown in Scheme 4. According to the proposed scheme the two ortho ring positions are not active in the direct intermolecular H/D exchange with MeOD, though they can slowly undergo an intramolecular exchange with the oxonium group. The suggested mechanism is consistent with the reactivity of protonated $Ph(CH_2)_3OMe$ towards MeOD showing the incorporation of just one D-atom. Due to the methyl substitution, the protonated ether oxygen is now too basic to engage in H^+/D^+ transfer processes with the ortho ring carbons.

The electrostatic stabilization gained by the interaction between the oxonium moiety and the phenyl ring appears to play a role when the aliphatic chain is longer than $n = 2$. Protonated **1** and **2** undergo complete dissociation upon CI(*i*-C_4H_{10}). Also the higher members, though, undergo dissociation to a certain extent upon CI(*i*-C_4H_{10}) and the question may rise whether the loss of water occurs from a folded conformation where the aromatic ring may provide nucleophilic assistance to C–O bond cleavage. In this case the $C_9H_{11}^+$, $C_{10}H_{13}^+$, and $C_{11}H_{15}^+$ ions formed by loss of water following the protonation reaction of **3**–**5** should have the structure of protonated indane, protonated tetraline, and protonated benzosuberane, respectively. The ions of interest have been sampled by the H/D exchange reaction comparing their reactivity behavior with the one observed for the predicted product ions. The model ions, the protonated benzocycloalkenes, react with MeOD by a sequence of five steps of H/D exchange occurring at comparable rates, if their statistical probability is accounted for (Table 4). The protonation sites are clearly the aromatic carbon atoms characterized by comparable values of site specific PA [30]. The

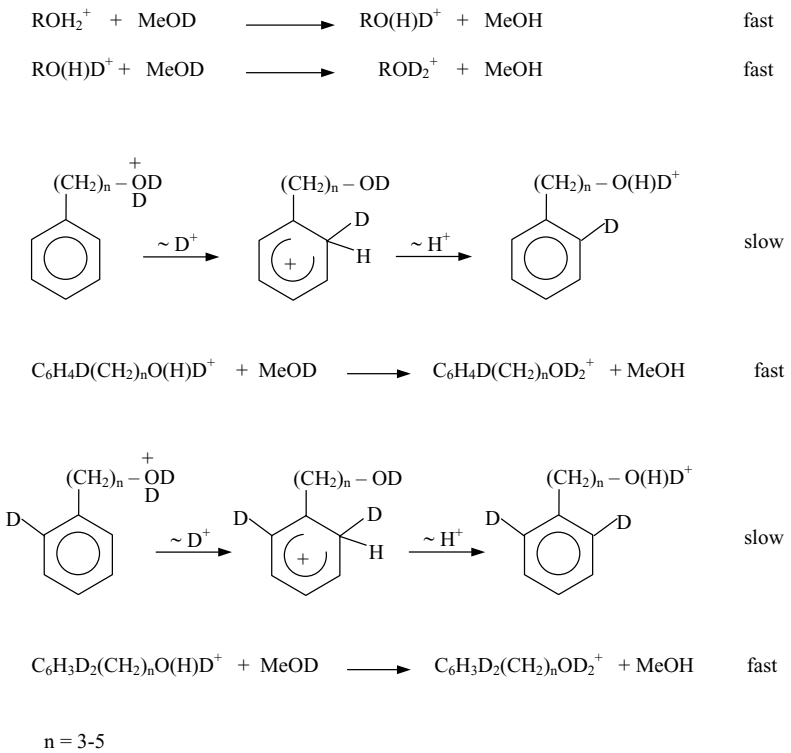

Scheme 4.

reactivity behavior of $C_{10}H_{13}^+$ and $C_{11}H_{15}^+$ ions obtained by CI(i-C_4H_{10}) of **4** and **5** matches well with the exchange reactivity displayed by the corresponding protonated benzocycloalkene, thus proving the occurrence of a cycloalkylation process. However, the $C_9H_{11}^+$ ions obtained from the CI(i-C_4H_{10}) of **3** are unreactive towards H/D exchange with MeOD, pointing to the formation of an isomeric structure different from protonated indane. It is likely that a linear side-chain benzyl-type cation is formed whose conjugate base is characterized by a PA high enough to make H/D exchange with methanol not accessible on thermodynamic grounds [25a,28]. The relative ease of ring closure reactions is known to depend on the size of the ring being formed, tuned by specific structural factors [31]. However, whereas the formation of tetraline by an intramolecular cycloalkylation reaction is reported, under similar Friedel–Crafts conditions only traces of indane are formed [32]. Noteworthily, the formation of tetraline from the radiolytic reaction of **4** is confirmed by the characterization of the ionic arenium intermediate by the H/D eschange reaction in FT–ICR, whereas the evidence is negative for a cyclized product from **3**. When **5** is the reagent, the product ion of an intramolecular cyclization process is observed only in the low pressure conditions of FT–ICR mass spectrometry, where the low density environment is unable to provide third body thermalization of any excited species or any kind of intermolecular ion-neutral interaction. Under these circumstances, processes may be activated that require surmounting activation energy barriers and take advantage of an intramolecular ion-neutral end group interaction.

5. Conclusion

The role of R_2OH^+–π and ROH_2^+–π interactions is clearly discernible in the alkylation and protonation reactions, respectively, of ω-phenylalkanols in the gas phase under two different pressure regimes, close to 1 atm in radiolytic systems and ca 10^{-8} mbar in FT–ICR mass spectrometry. The active site for the alkylation and the protonation processes is found to be the oxygen atom, reflecting the operation of both kinetic and thermodynamic factors. The ensuing ionic intermediates, $RO(H)E^+$ (E = H, Me, Me_3C), show a reactivity behavior that can be accounted for by the varying length of the aliphatic chain. In the radiolytic experiments, where the high pressure environment ensures a high frequency of thermalizing collisions, the methylated intermediates, $RO(H)Me^+$, are deprotonated by an added base yielding the corresponding methyl ether as the neutral product. In competition with the deprotonation reaction, ions $RO(H)Me^+$ of the lower homologues (**1**, **2**) may undergo nucleophilic attack by a second molecule of ROH to give a symmetric ether. The efficiency of this reaction increases with the decreasing length of the alkyl chain and with increasing temperature. No evidence for products of nucleophilic attack was found from the higher homologues (**3**–**5**), even at higher temperature. This result is suggestive of a higher stability of these ions, which may attain a configuration allowing an intramolecular hydrogen bond between the OH^+ end and the π-electrons of the phenyl ring. Similar considerations can explain the results of CI(i-C_4H_{10}) experiments yielding the intact protonated species only in the case of **3**–**5**, where the aliphatic chain contains three or more methylene units. The oxonium intermediates from **3**–**5** may in fact benefit from the electrostatic stabilization afforded by the approach of the oxonium moiety to the phenyl ring. The folding of the aliphatic chain is highlighted by the formation of protonated tetraline from **4**, as a result of an intramolecular nucleophilic attack. The folding is driven by the quest for electrostatic stabilization by the positively charged oxonium end. In fact the situation appears to be quite different in the neutral ω-phenylalkanols. The role and extent of OH–π type intramolecular hydrogen bond within neutral **1**–**3** has been studied and debated by various spectroscopic methods showing a limited contribution of H-bonded conformers [33].

It may be finally remarked that cation–π interactions may be profitably studied in the gas phase, operating in an environment void of the complicating factors such as the presence of counterions and solvent that can profoundly affect their extent and relative weight with respect to other non-covalent interactions [6,34].

Acknowledgements

This work was supported by the Italian Ministero dell'Istruzione, dell'Università e della Ricerca.

References

[1] (a) J.C. Ma, D.A. Dougherty, Chem. Rev. 97 (1997) 1303;
(b) D.A. Dougherty, Science 271 (1996) 1163;
(c) J.P. Gallivan, D.A. Dougherty, Proc. Natl. Acad. Sci. U.S.A. 96 (1999) 9459.
[2] (a) I. Alkorta, I. Rozas, J. Elguero, Chem. Soc. Rev. 27 (1998) 163;
(b) M. Meot-Ner, C. Deakyne, J. Am. Chem. Soc. 107 (1985) 469.
[3] (a) Y. Mo, G. Subramanian, J. Gao, D.M. Ferguson, J. Am. Chem. Soc. 124 (2002) 4832;
(b) D.L. Beene, G.S. Brandt, W. Zhong, N.M. Zacharias, H.A. Lester, D.A. Dougherty, Biochemistry 41 (2002) 10262.
[4] J.W. Gokel, L.J. Barbour, R. Ferdani, J. Hu, Acc. Chem. Res. 35 (2002) 878.
[5] H.S. Choi, S.B. Suh, S.J. Cho, K.S. Kim, Proc. Natl. Acad. Sci. U.S.A. 95 (1998) 12094.
[6] J.P. Gallivan, D.A. Dougherty, J. Am. Chem. Soc. 122 (2000) 870.
[7] J.B. Nicholas, B.P. Hay, D.A. Dixon, J. Phys. Chem. A 103 (1999) 1394.
[8] (a) G.K. Koyanagi, D.K. Bohme, Int. J. Mass Spectrom. 227 (2003) 563;
(b) J. Amicangelo, P.B. Armentrout, J. Phys. Chem. A 104 (2000) 11420;
(c) A. Gapeev, C.-N. Yang, S.J. Klippenstein, R.C. Dunbar, J. Phys. Chem. A 104 (2000) 3246;

(d) A. Gapeev, R.C. Dunbar, J. Am. Chem. Soc. 123 (2001) 8360;
(e) T. Shoeib, A. Cunje, A.C. Hopkinson, K.W.M. Siu, J. Am. Soc. Mass Spectrom. 13 (2002) 408;
(f) O.M. Cabarcos, C.J. Weinheimer, J.M. Lisy, J. Chem. Phys. 110 (1999) 8429;
(g) P. Burk, I.A. Koppel, R. Kurg, J.-F. Gal, P.-C. Maria, M. Herreros, R. Notario, J.-L.M. Abboud, F. Anvia, R.W. Taft, J. Phys. Chem. A 104 (2000) 2824.
[9] R.L. Wooden, J.L. Beauchamp, J. Am. Chem. Soc. 100 (1978) 501.
[10] J. Sunner, K. Nishizawa, P. Kebarle, J. Phys. Chem. 85 (1981) 1814.
[11] (a) E. Cubero, F.J. Luque, M. Orozco, Proc. Natl. Acad. Sci. U.S.A. 95 (1998) 5976;
(b) H. Basch, W.J. Stevens, Theochem 338 (1995) 303.
[12] O. Mó, M. Yáñez, J.-F. Gal, P.-C. Maria, M. Decouzon, Chem. Eur. J. 9 (2003) 4330.
[13] (a) D. Heidrich, Angew. Chem. Int Ed. 41 (2002) 3208;
(b) P.C. Miklis, R. Ditchfield, T. A Spencer, J. Am. Chem. Soc. 120 (1998) 10482;
(c) D. Kuck, Mass Spectrom. Rev. 9 (1990) 583;
(d) S. Fornarini, M. E Crestoni, Acc. Chem. Res. 31 (1998) 827;
(e) D. Berthomieu, V. Brenner, G. Ohanessian, J.P. Denhez, P. Millié, H.E. Audier, J. Phys. Chem. 99 (1995) 712.
[14] (a) Y.L. Lee, S.L. Lee, H.S. Choi, S.J. Cho, K.S. Kim, T.-K. Ha, Chem. Phys Lett. 232 (1995) 67;
(b) S.Y. Jon, J. Kim, M. Kim, S.-H. Park, W.S. Jeon, J. Heo, K. Kim, Angew. Chem. Int. Ed. 40 (2001) 2116.
[15] (a) I. Rozas, I. Alkorta, J. Elguero, J. Phys. Chem. A 101 (1997) 9457;
(b) H. Adams, K.D.M. Harris, G.A. Hembury, C.A. Hunter, D. Livingstone, J.F. McCabe, Chem. Commun. (1996) 2531;
(c) M. Mons, I. Dimicoli, B. Tardivel, F. Piuzzi, V. Brenner, P. Milliè, Phys. Chem. Chem. Phys. 4 (2002) 571;
(d) R.N. Pribble, A.W. Garrett, K. Haber, T.S. Zwier, J. Chem. Phys. 103 (1995) 531;
(e) T. Steiner, G. Koellner, J. Mol. Biol. 305 (2001) 535;
(f) T. Steiner, Biophys. Chem. 95 (2002) 195.
[16] E.S. Kryachko, M.T. Nguyen, J. Phys. Chem. A 105 (2001) 153.
[17] (a) B. Chiavarino, M.E. Crestoni, S. Fornarini, D. Kuck, J. Phys. Chem. A 107 (2003) 4619;
(b) M.E. Crestoni, S. Fornarini, D. Kuck, J. Phys. Chem. 99 (1995) 3150;
(c) M.E. Crestoni, S. Fornarini, D. Kuck, J. Phys. Chem. 99 (1995) 314;
(d) S. Fornarini, Mass Spectrom. Rev. 15 (1996) 365.
[18] F. Cacace, Acc. Chem. Res. 21 (1988) 215.
[19] A.G. Marshall, C.L. Hendrickson, G.S. Jackson, Mass Spectrom. Rev. 17 (1998) 1.
[20] J.E. Bartmess, R.M. Georgiadis, Vacuum 33 (1983) 149.
[21] T. Su, W.J. Chesnavich, J. Chem. Phys. 76 (1982) 5183.
[22] M.E. Crestoni, J. Phys. Chem. 97 (1993) 6197, and references therein.
[23] J.B. Nicoll, D.V. Dearden, KinFit, 1.0 ed. Department of Chemistry and Biochemistry, A.Brigham Young University, Provo, UT, 1997.
[24] (a) T.B. McMahon, T. Heinis, G. Nicol, J.K. Hovey, P. Kebarle, J. Am. Chem. Soc. 110 (1988) 7591;
(b) M.N. Glukhovtsev, J.E. Szulejko, T.B. McMahon, J.W. Gauld, A.P. Scott, B.J. Smith, A. Pross, L. Radom, J. Phys Chem. 98 (1994) 13099.
[25] (a) E.P. Hunter, S.G. Lias, in: W.G. Mallard, P.J. Linstrom (Eds.), Proton Affinity Evaluation In NIST Chemistry WebBook, NIST Standard Reference Database Number 69, National Institute of Standards and Technology, Gaithersburg MD, March 2003 (http:www.//webbook.nist.gov);
(b) M. Eckert-Maksic, M. Klessinger, Z.B. Maksic, J. Phys. Org. Chem. 8 (1995) 435.
[26] D.K. Sen Sharma, P. Kebarle, J. Am. Chem. Soc. 104 (1982) 19.
[27] D. Kuck, Int. J. Mass Spectrom. Ion Processes 117 (1992) 441.
[28] (a) M. Kirk Green, C.B. Lebrilla, Mass Spectrom. Rev. 16 (1997) 53;
(b) S.J. Lias, Phys. Chem. 88 (1984) 4401.
[29] (a) B.S. Freiser, R.L. Woodin, J.L. Beauchamp, J. Am. Chem. Soc. 97 (1975) 6983;
(b) D. Kuck, S. Ingemann, L. de Koning, H.-F. Grützmacher, N.M.M. Nibbering, Angew. Chem. Int. Ed. 24 (1985) 693;
(c) J. Ni, A.G. Harrison, Can. J. Chem. 73 (1995) 1779.
[30] M. Eckert-Maksic, Z.B. Maksic, M. Klessinger, J. Chem. Soc. Perkin Trans. 2 (1994) 285.
[31] L. Mandolini, Adv. Phys. Org. Chem. 22 (1986) 1.
[32] R.M. Roberts, A.A. Khalaf (Eds.), Friedel-Crafts Alkylation Chemistry, Marcel Dekker, New York, 1984, p. 579.
[33] (a) M. Mons, E.G. Robertson, J.P. Simons, J. Phys. Chem. A 104 (2000) 1430;
(b) N. Guchhait, T. Ebata, N. Mikami, J. Am. Chem. Soc. 121 (1999) 5705.
[34] S. Bartoli, S. Roelens, J. Am. Chem. Soc. 121 (1999) 11908.